$CuBi_2O_4$: electronic structure, optical properties, and PEC performance limitations of the photocathode

Jason K. Cooper,[,1,2] Zemin Zhang,[1,8] Subhayan Roychoudhury,[3,5] Chang-Ming Jiang,[1] Sheraz Gul,[6] Yi-Sheng Liu,[3] Rohan Dhall,[4,5] Alejandro Ceballos,[7] Junko Yano,[1,6] David Prendergast,[5] Sebastian E. Reyes-Lillo[9,*]*

[1]Joint Center for Artificial Photosynthesis, [2]Chemical Sciences Division, [3]Advanced Light Source,

[4]National Center for Electron Microscopy, [5]The Molecular Foundry, [6]Molecular Biophysics and

Integrated Bioimaging Division, Lawrence Berkeley National Laboratory, Berkeley, California 94720,

United States

[7]Department of Physics, University of California, Berkeley, Berkeley, CA 94720

[8]School of Physical Science and Technology, Lanzhou University, Lanzhou 730000, China

[9]Departamento de Ciencias Físicas, Universidad Andres Bello, Santiago 837-0136, Chile

* Corresponding Author: jkcooper@lbl.gov, sebastian.reyes@unab.cl

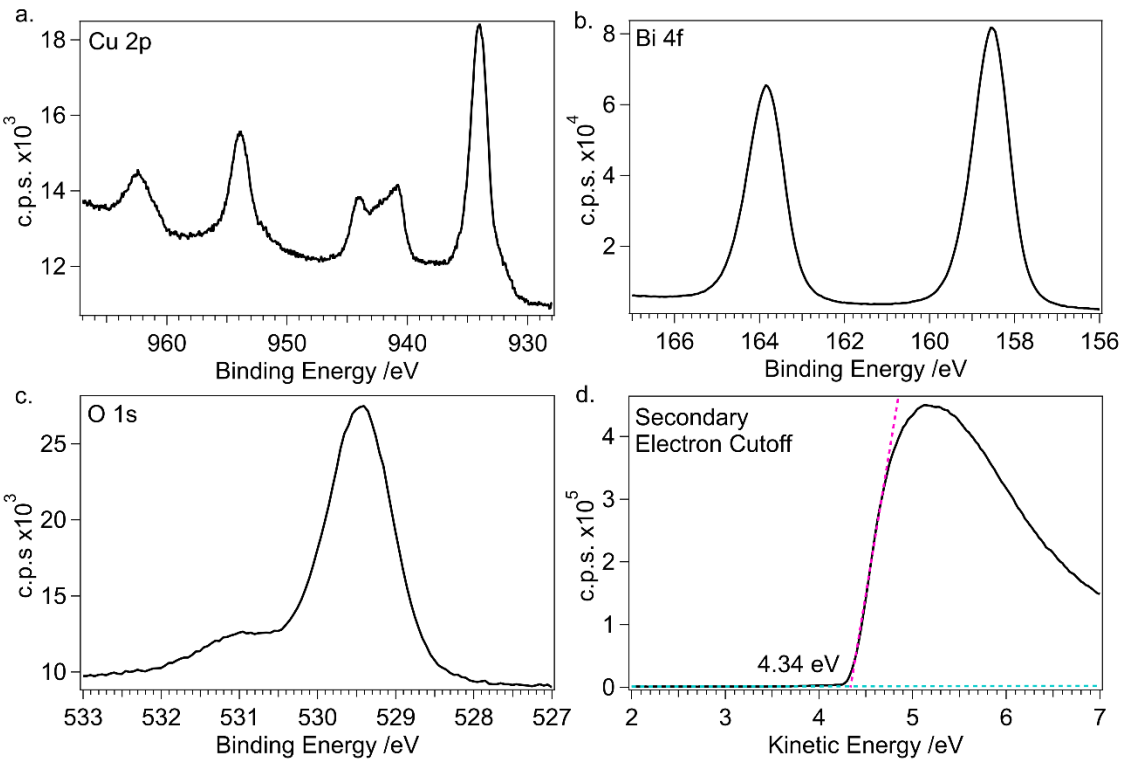

Figure S1. X-ray photoelectron spectra of $CuBi_2O_4$ for a.) Cu 2p, b.) Bi 4f, c.) O 1s, and d.) the secondary electron cutoff (also collected with monochromic Al K_α) showing the work function is 4.34 eV.

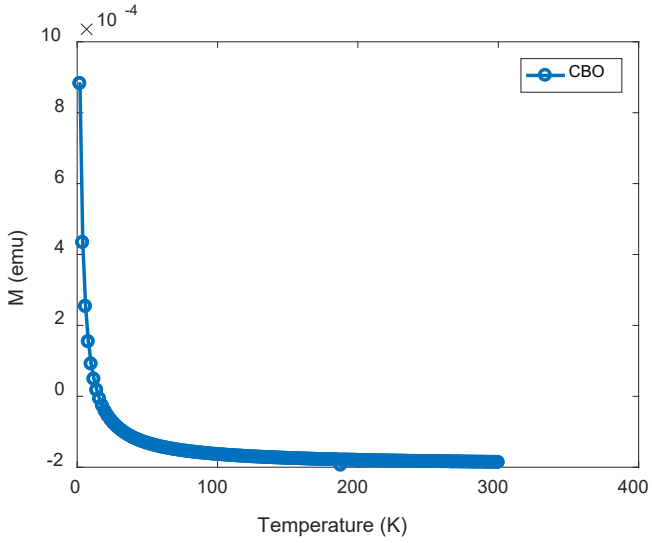

Figure S2. Temperature dependent magnetic field strength measured by SQUID (superconducting quantum interference device) magnetometry.

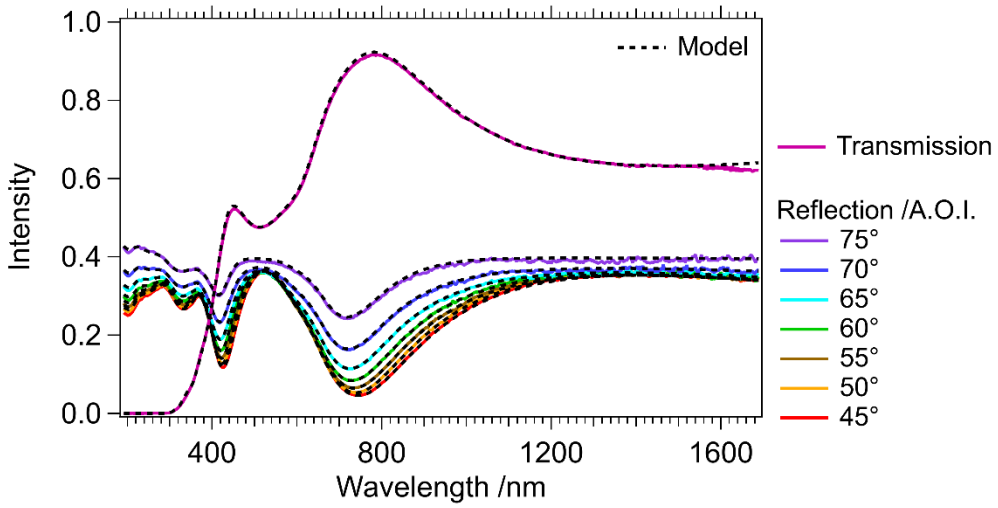

Figure S3. Transmission and reflection intensity at several angles of incidence measured relative to the surface normal of $CuBi_2O_4$ (157 nm thick) on fused silica substrate measured with the variable angle spectroscopic ellipsometry (VASE) instrument. Included is the modeled data based on the ellipsometry model using the oscillators described in Table S1.

Table S1. P-semi parameters used for fitting variable angle spectroscopic ellipsometry of $CuBi_2O_4$.

Type	Position /eV	Broadening /eV	Amplitude
PSemi-M0	1.50	0.174	0.036
PSemi-M0	1.99	0.105	0.569
PSemi-M0	2.31	0.258	0.284
PSemi-M0	2.92	0.197	0.542
PSemi-Tri	3.47	0.118	1.792
PSemi-Tri	3.74	0.128	1.309
PSemi-Tri	4.35	0.208	5.801
PSemi-Tri	5.48	0.043	0.980
PSemi-Tri	6.81	0.463	1.021

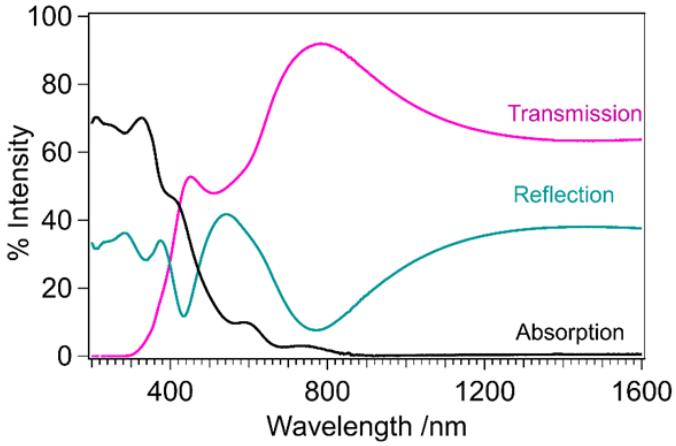

Figure S4. Reflection, transmission, and absorption spectra of the $CuBi_2O_4$ (157 nm) on fused silica.

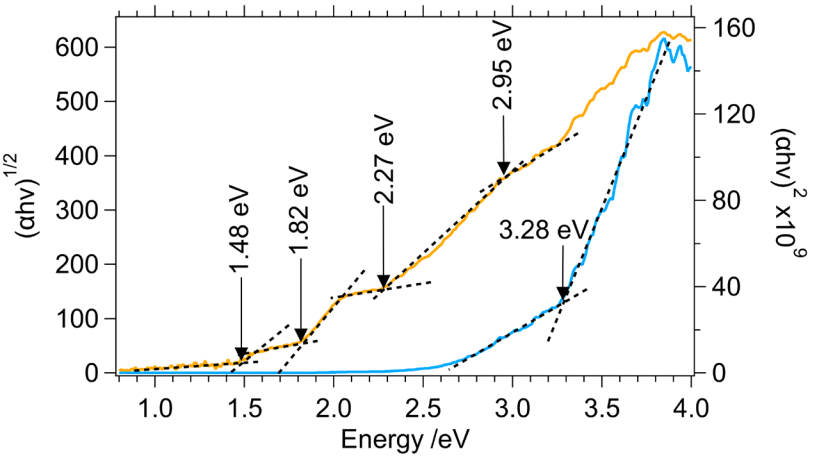

Figure S5. Tauc plots for indirect and direct bandgap analysis based on the photothermal deflection spectrum of the $CuBi_2O_4$ (157 nm) on fused silica. Included is analysis of the inflection points in the data corresponding to the introduction of a new optical component to the absorption spectrum indicating the location of several indirect and direct transitions.

Table S2 shows the magnetic configurations considered in this work: anti ferromagnetic with spins aligned along the c-axis and anti-aligned along the a-b plane (AFM-C), anti-ferromagnetic with spin anti-aligned along the c-axis and aligned parallel along the a-b plane (AFM-A), anti-ferromagnetic with spins anti-aligned along c-axis and a-b plane (AFM-G), ferromagnetic (FM), and nonmagnetic (NM). For HSE, we find that AFM- C is the lowest energy structure, in good agreement with the experimental results.[1]

The computed lattice parameters for AFM-C are in good agreement with the experimental lattice parameters a = b = 8.499 Å and c= 5.817 Å. The HSE in-plane (out-of-plane) lattice parameters under- (over-) estimate experimental values by 0.8% (0.6%). In addition, HSE computed O-Cu-O angles 175.2° underestimates experimental values 176.2° by only 0.6°.

Table S2: Total-energy per formula unit (meV/f.u.) and lattice parameters (Å) for the magnetic configurations considered in this work. Full structural relaxations are performed using the DFT+U method with a Hubbard U of 7 eV and the HSE hybrid functional with a mixing parameter of 25%.

	DFT+U (U=7 eV)		HSE	
Magnetic phase	Energy (meV/f.u.)	Lattice Param. (Å)	Energy (meV/f.u.)	Lattice Param. (Å)
AFM-C	0.2	a=b=8.494, c=6.025	0	a=b=8.429, c=5.851
AFM-A	5.1	a=b=8.497, c=6.023	4.1	a=b=8.427, c=5.851
AFM-G	0	a=b=8.494, c=6.024	0.1	a=b=8.427, c=5.851
FM	5.1	a=b=8.495, c=6.025	4.9	a=b=8.425, c=5.854
NM	645.3	a=b=8.463, c=6.011	287.1	a=b=8.422, c=5.852

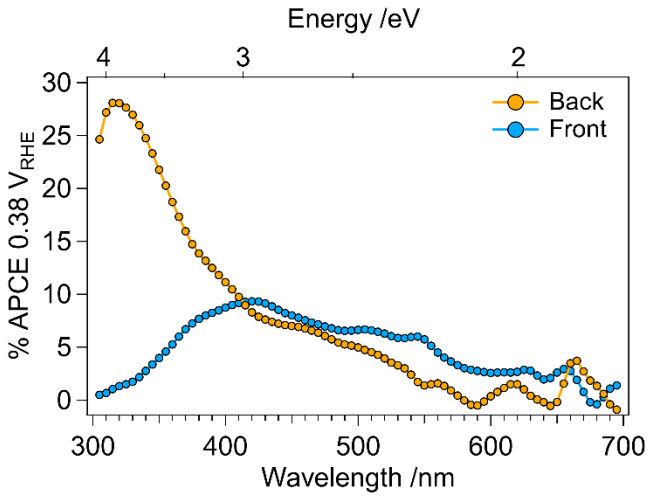

Figure S6. Absorbed photon to current efficiency (APCE) of a 160 nm thick $CuBi_2O_4$ sample on ITO glass tested in 0.1 M $KHCO_3$ with 0.5 M $Na_2S_2O_8$.

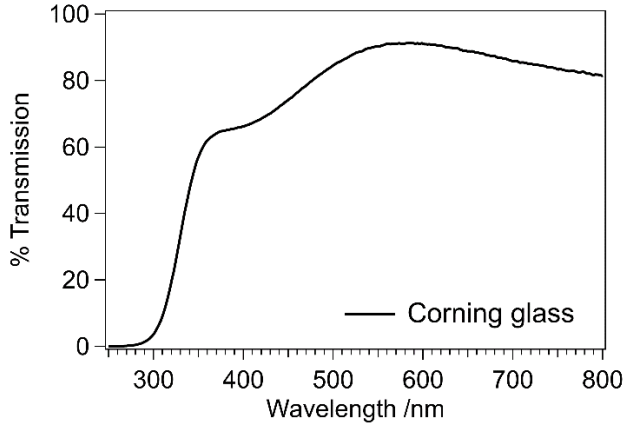

Figure S7. Transmission spectrum of the Corning boro-aluminosilicate glass substrate used in the IPCE and PEC testing.

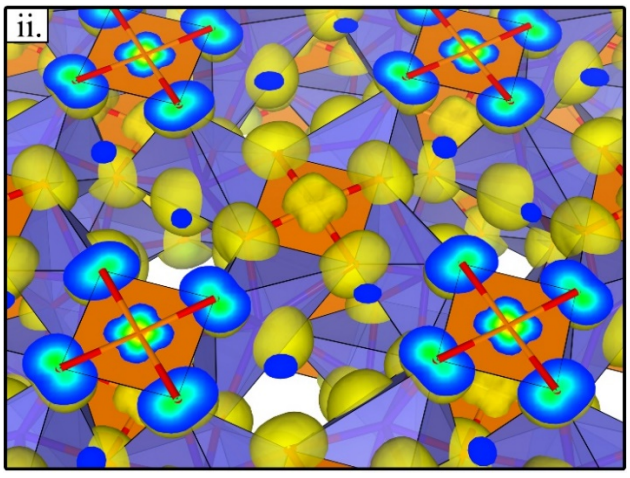

Figure S8. Integrated local density of states of region ii. (Figure 4) showing the Bi 6s, Cu $3d_{xy}$ / O sp^3 orbitals.

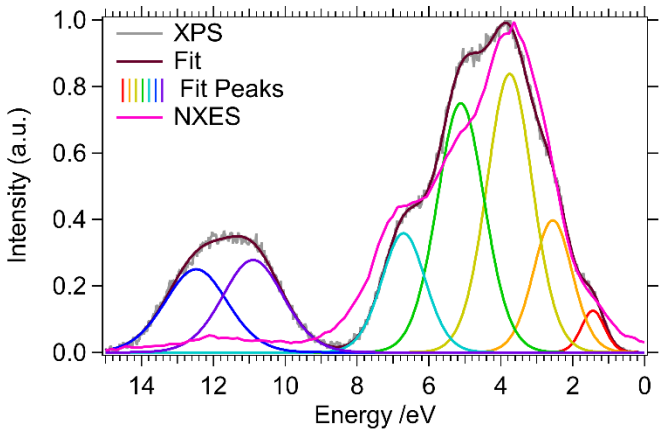

Figure S9. X-ray photoelectron valence band spectrum of $CuBi_2O_4$ shown with multi-gaussian fit components which are correlated to the 5 orbital regions revealed by DFT (Figure 4a) above 8 eV with the remaining two related to Bi 6s states, similar to $BiVO_4$. Also included is the normal X-ray emission spectrum (NXES) aligned to the same energy axis as the XPS data also demonstrating the same 5 spectral components above 8 eV.

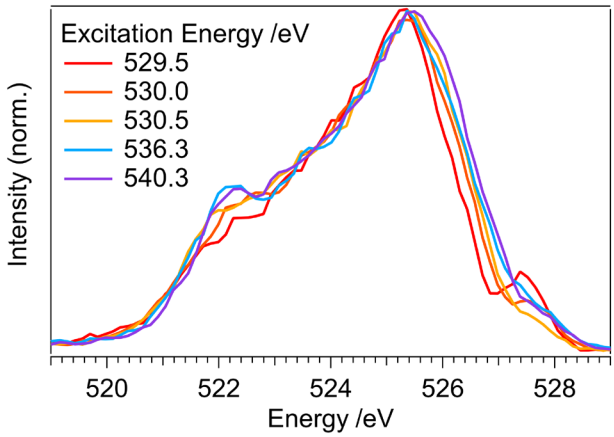

Figure S10. Intensity normalized X-ray emission spectra collected with resonant excitation (indicated).

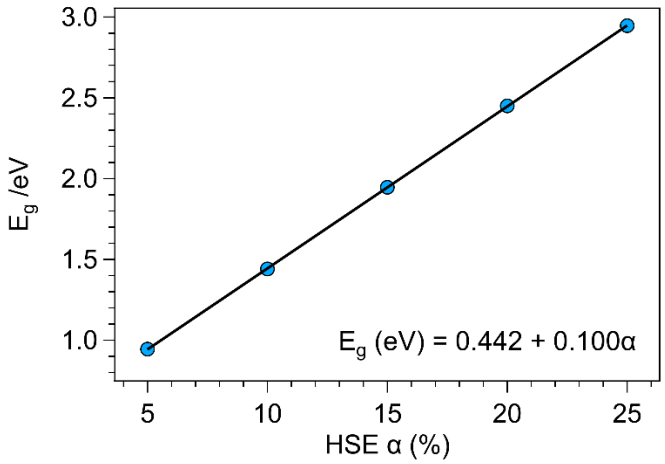

Figure S11. Partial density of state HSE band gap as a function of the value of the Hartree-Fock mixing parameter. The value of the mixing parameter is adjusted to 10.6% to match the measured optical gap (1.5 eV).

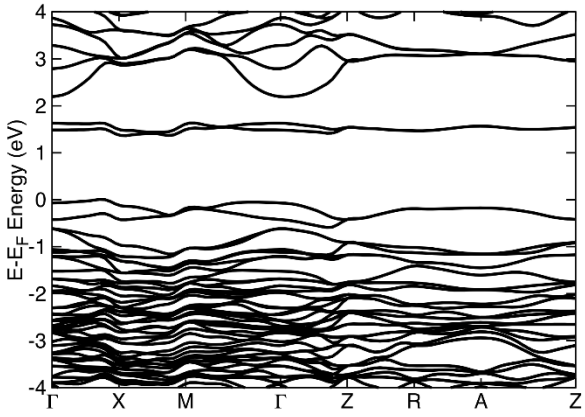

Figure S12. Band structure calculation computed with HSE and a Hartree-Fock mixing parameter of 10.6%. The indirect band gap is sustained between the the Γ-X and X-M segments. The Fermi level is set to the highest occupied band.

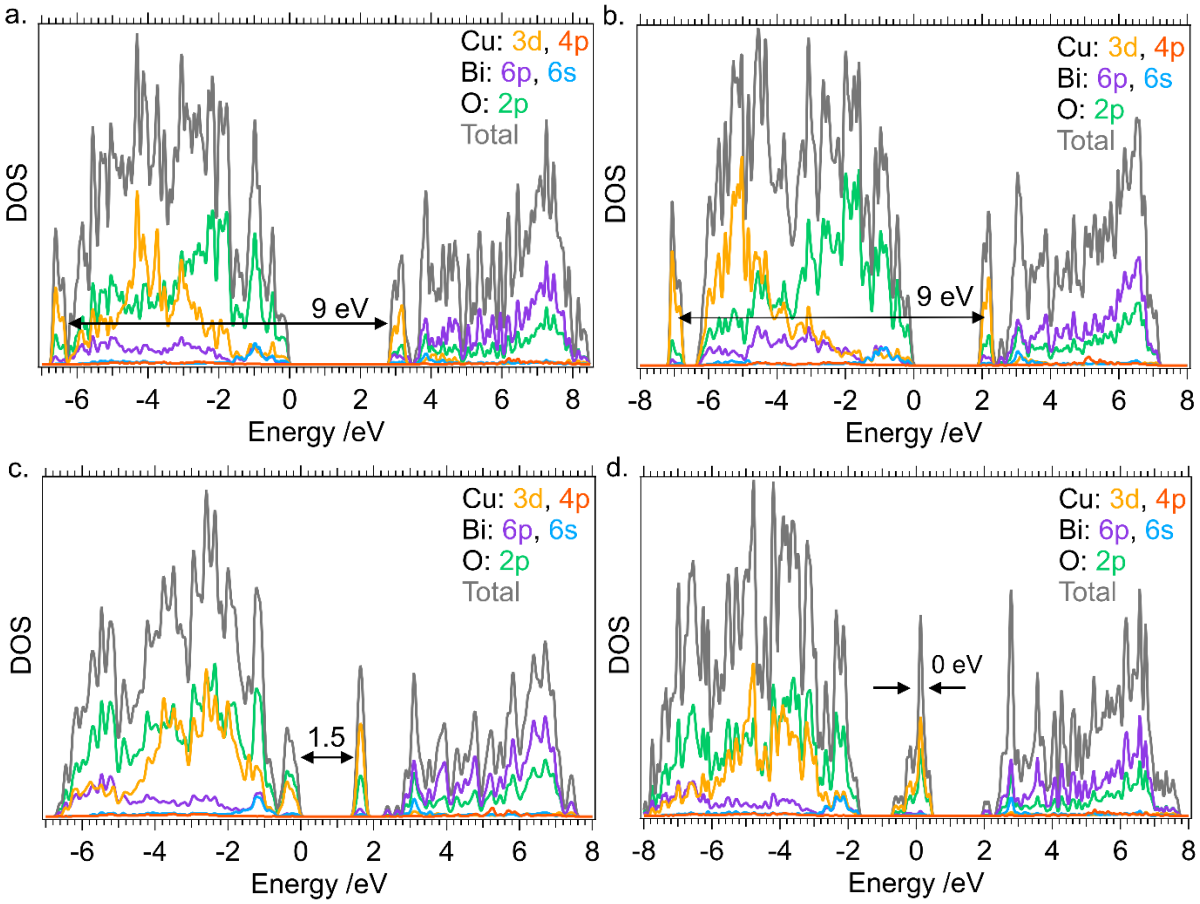

Figure S13. Partial density of states calculated using a.) HSE for the AFM-C configuration with 25% mixing, b.) DFT+U for the AFM-C using U = 7 eV, c.) HSE for the AFM-C configuration with 10.6% mixing, and d.) HSE for the NM configuration with spin turned-off. In all AFM-C calculations, spin-up and spin-down channels are equal and lead to a local spin magnetization of approximately 0.7 μ_B in each Cu-ion.

Table S3. Gaussian peak parameters used for fitting the XAS data shown in Figure 5b. Background spline: base = 0, max = 1, xhalf = 543.5 – 5.89 eV, rate = 0.35 eV

Peak Number	Location /eV	Amplitude	Area	FWHM /eV
i	535.69	0.56	0.51	0.85
ii	537.31	3.20	5.72	1.68
iii	538.30	0.52	0.52	0.94
iv	539.55	2.80	5.46	1.83
v	540.99	1.40	2.32	1.56
vi	542.14	0.97	1.82	1.76
vii	544.25	0.06	0.04	0.69
viii	546.38	0.62	2.01	3.06
ix	549.54	0.06	0.08	1.24
x	551.47	0.19	1.22	6.01

REFERENCES

1. Yamada, K.; Takada, K.-i.; Hosoya, S.; Watanabe, Y.; Endoh, Y.; Tomonaga, N.; Suzuki, T.; Ishigaki, T.; Kamiyama, T.; Asano, H.; Izumi, F., Three-Dimensional Antiferromagnetic Order and Anisotropic Magnetic Properties in Bi_2CuO_4. *J. Phys. Soc. Jpn.* **1991,** *60* (7), 2406-2414.